ACADEMIC PRESS

Available online at www.sciencedirect.com
SCIENCE DIRECT®

Journal of Catalysis 218 (2003) 24–31

JOURNAL OF CATALYSIS

www.elsevier.com/locate/jcat

Kinetic study of the hydrodenitrogenation of carbazole over bulk molybdenum carbide

Agnieszka Szymańska,[a,c] Marek Lewandowski,[a] Céline Sayag,[b] and Gérald Djéga-Mariadassou [b,*]

[a] *Institute of Coal Chemistry of PAN, Sowińskiego 5, 44-121 Gliwice, Poland*
[b] *Laboratoire Réactivité de Surface, UMR CNRS 7609, casier 178, Université P. & M. Curie, 4 Place Jussieu, 75252 Paris Cedex 05, France*
[c] *Silesian Technical University in Gliwice, Department of Chemistry, M. Strzody 9, 44-100 Gliwice, Poland*

Received 10 July 2002; revised 7 November 2002; accepted 17 February 2003

Abstract

Hydrodenitrogenation (HDN) of N-containing compounds (carbazole in this paper) in the presence of a small amount of sulfur (50 ppm) requires a strong catalytic hydrogenating function. Bulk molybdenum carbide, Mo_2C, behaves like a noble metal and has strong hydrogenating properties and can catalyse deep HDN if the S content is not too high. A kinetic investigation monitored both the hydrogenating function through carbazole consumption and the HDN of carbazole through two kinetically coupled cycles. Biphenyl was not observed. Kinetic coupling occurs by means of adsorbed orthocyclohexylaniline. The first route is the direct HDN reaction, leading to cyclohexylbenzene, while the second hydrogenation route leads to bicyclohexyl. At 633 K, a zero-order reaction is observed with respect to carbazole; total HDN is observed for 0.4 s, and the selectivity ratio of bicyclohexyl to cyclohexylbenzene is equal to 9.

Keywords: Molybdenum carbide; Hydrodenitrogenation; Carbazole

1. Introduction

Hydrotreating processes, such as hydrodenitrogenation (HDN) and hydrodesulfurization (HDS), are the main processes leading to the removal of nitrogen- (N-) and sulfur- (S-) containing compounds present in petroleum feedstocks, respectively. The demand for cleaner fuels is growing (S < 50 ppm for 2005), and even if the activity of conventional hydrotreating catalysts (alumina-supported sulfided NiMo–CoMo) has improved considerably in recent years, a limit seems to have been reached. The latter catalysts are hardly active towards refractory molecules. A two-stage hydrotreating process could be considered using highly active hydrotreating catalysts that possess noble metal properties and are tolerant to small amounts of S-containing compounds. A recent review by Prins [1] emphasises the mechanisms of HDN and discusses the recently introduced transition-metal carbide and nitride catalysts.

Transition-metal carbides and nitrides have been studied intensively for more than a decade; it has been shown that they may be excellent potential substitutes for hydrotreating catalysts [2–6]. Among them, molybdenum nitrides and carbides stand out because they are more active than commercial alumina-supported sulfided NiMo and CoMo catalysts, both in HDN or HDS of simple model molecules [3,7–9] and even in the removal of nitrogen from coal-derived liquids [10]. Schlatter et al. [3] were the first to report that unsupported molybdenum nitrides exhibit a much higher selectivity towards aromatic products during the HDN of quinoline than sulfided NiMo supported on alumina and, therefore, lead to lower hydrogen consumption. Lee et al. [8] reported that bulk γ-Mo_2N was more active for the C–N hydrogenolysis of 1,2,3,4-tetrahydroquinoline to 2-propylbenzene during the HDN of quinoline under atmospheric pressure than a sulfided Ni–Mo/Al_2O_3 catalyst. Choi et al. [7] studied the HDN of pyridine over γ-Mo_2N at higher pressure and reported that the molybdenum nitride was more active than a sulfided CoMo/Al_2O_3 catalyst, with a higher selectivity to C–N bond hydrogenolysis.

* Corresponding author.
E-mail address: djega@ccr.jussieu.fr (G. Djéga-Mariadassou).

0021-9517/03/$ – see front matter
doi:10.1016/S0021-9517(03)00072-1

Moreover, these metal nitrides were shown to be sulfur-resistant [10,11].

These catalysts can also be supported on oxides such as alumina [12–15] or on carbonaceous supports [16–18] and still behave similarly in hydrotreating reactions to the bulk catalysts [12,17]. However, the pore size distribution of the supported catalysts must be carefully designed to enable the large N- or S-containing molecules to reach the active sites [19].

It is well known that the HDN reaction is more difficult than the HDS reaction, the C–N bond energy being higher than that of the C–S bond energy. Furthermore, nitrogen removal requires ring hydrogenation prior to the C–N bond cleavage [20]. Perot [21] assumed that, during HDN processes over commercial catalysts (alumina-supported sulfided NiMo and CoMo), three types of reactions occur, leading to the hydrogenolysis of nitrogen compounds: (i) hydrogenation of nitrogen heterocycles, (ii) hydrogenation of benzenic cycles, and (iii) C–N bond cleavage. Therefore, bifunctional catalysts with both hydrogenating and hydrogenolysing active centres are necessary. Another mechanism, such as cracking, can be observed over oxides (MoO_3, NiO), as indicated by Ledoux et al. [22].

Much less attention has been paid to carbides and nitrides in the study of the HDN of heavier N-containing hydrocarbons such as carbazole, which is representative of refractory N-containing components of heavy fractions derived from petroleum. The only publications thus far are those by Nagai and co-workers [4,23]. They studied alumina-supported molybdenum carbide and nitride for the HDN of carbazole *in the absence of sulfur*. They observed higher activity of the carbides than of the corresponding nitrides or sulfides. N-containing compounds are usually very strong inhibitors of HDS reactions over alumina-supported sulfided Ni–Mo or Co–Mo catalysts [24–26] as well as over molybdenum carbide [27]. Therefore, the kinetic parameters for both HDN and HDS reactions should be established over molybdenum carbides.

The present work is concerned with the activity and selectivity of the HDN of carbazole over bulk molybdenum carbide in the presence of 50 ppm of sulfur introduced as dimethyldisulfide into the feed to simulate the operating conditions of a second-stage hydrotreating process. Investigations were performed at a wide range of conversions (from 10 to 100%) and temperatures, which enable us to describe the kinetics of the HDN reaction of carbazole as well as the activity and selectivity to bicyclohexyl of the bulk molybdenum carbide versus contact time.

2. Experimental

2.1. Catalyst

MoO_3 (Fluka, $\geqslant 99.5\%$) was used as the precursor for the catalyst synthesis. The gases used were dihydrogen (H_2, Air Liquide, Custom grade C, purity > 99.995%), helium (He, Air Liquide, Custom grade C, purity > 99.995%), dioxygen (O_2, Air Liquide, Custom grade C, purity > 99.5%), and methane (CH_4, Air Liquide, Custom grade N30, purity > 99.9%).

Carbazole (Fluka, 98%), *o*-xylene (Fluka, $\geqslant 98\%$), and dimethyldisulfide (Fluka, $\geqslant 98\%$) were used as reactants for the kinetic study.

Molybdenum carbide was prepared according to a modified standard procedure of Volpe and Boudart [28]. Molybdenum trioxide (3 g) was placed on a porous disc in a quartz reactor and carburized with a mixture of 10 vol% CH_4/H_2, at a volume hourly space velocity (VHSV) of about 85 h^{-1}. The temperature was increased linearly from 300 to 973 K at a rate of 53 K h^{-1} and was kept at 973 K for 1 h. Finally, the sample was cooled to room temperature (RT) in the reactant carburizing carrier gas. When exposure to air was necessary, the sample was passivated with a 1 vol% O_2/He gas mixture to form a protective oxygen layer on its surface.

2.2. Characterization

Structural characterization of the molybdenum carbide was carried out by X-ray diffraction (XRD) using a SIEMENS D-500 automatic diffractometer with Cu-K_α monochromatized radiation. The degree of crystallinity of the obtained carbides was estimated from the intensity of all reflections in the 2θ range from 10° to 90°.

High-resolution transmission electron microscopy (HRTEM) was carried out on fresh and used carbides. The HRTEM study was performed using a JEOL 200 CX electron microscope. A Quantachrome-Quantasorb Jr apparatus was used for the surface area (*Sg*) measurement under dynamic conditions. The *Sg* of the catalyst was obtained from the nitrogen adsorption/desorption at different partial pressures of nitrogen. A standard *Sg* measurement using the BET method was based on a three-point analysis consisting of mixtures of 10, 20, and 30 vol% N_2/He. The material (100 mg) was outgassed in a nitrogen stream at 623 K for 2 h before measurement.

CO uptake is a classical technique used to titrate the metallic sites. Therefore, it is also widely used to titrate the active sites of transition-metal carbide or nitrides [3,28–32]. The CO uptake was performed in situ, i.e., in the synthesis reactor without exposing the fresh carbide to air or to the passivating mixture. Pulses of a known quantity of CO (17 µmol) were injected at regular intervals into the sample at RT in a stream of He (40 mL min^{-1}) purified by an oxygen trap (Oxysorb, Messer Griesheim). After each injection, the quantity of probe molecules that were not chemisorbed was measured using a conventional device equipped with a TCD. Injections were continued until the sites were saturated with CO. Data were processed and the number of micromoles of CO chemisorbed per gram of sample was determined.

2.3. Kinetic study of HDN of carbazole

The HDN of carbazole was conducted with a down-flow fixed-bed microreactor in a high-pressure flow system. All catalytic runs were performed in the presence of a small amount of sulfur (50 ppm S), produced by the decomposition of 70 ppm of dimethyldisulfide (DMDS) added to the feed. The catalyst (density = 1.5 g cm^{-3}, weight = 0.6 g, grain size 0.25–0.315 mm) was mixed with carborundum (SiC) at a ratio of catalyst to SiC = 1/5. The liquid feed, consisting of 0.4 wt% carbazole in *o*-xylene, was fed to the reactor by means of a high-pressure piston pump (Gilson model 307). The hydrogen flow (30 to 360 cm^3 min^{-1}) and total pressure were controlled by a mass flow controller (Brooks 5850TR) and a back-pressure regulator (Brooks 5866), respectively. The temperature of the oven was regulated using a temperature controller (Hamyoung MX9).

The kinetic study was carried out at a total pressure of 6 MPa at temperatures between 553 and 653 K, with a H_2/feed volumic ratio of 600 and contact times (t_c) ranging from 0.07 to 0.8 s. The contact time (t_c) was defined as follows: t_c (s) = catalyst volume (cm^3)/(H_2 flow + feed flow) (cm^3 s^{-1}). The liquid products of the reaction were collected every hour in the condenser maintained at 288 K. Finally, this liquid was analyzed by gas chromatography (HP 4890) using a capillary column (HP1, 30 m × 0.25 mm × 0.25 µm) and a FID detector. The product identification was confirmed by both GCMS analysis (Finnigat Mat Model 800, capillary column DB5, 30 m × 0.25 mm × 0.25 µm and HP5890-HP5971A, capillary column PONA, 50 m × 0.20 mm × 0.5 µm) and injection of the standards. At each temperature, the molybdenum carbide was stabilized in situ for 10 h with a mixture of 70 ppm of DMDS/*o*-xylene in the hydrogen carrier gas (60 mL min^{-1}) at the temperature of the process and at a total pressure of 6 MPa. The catalyst did not exhibit deactivation versus time of run throughout the whole kinetic study.

3. Results and discussion

3.1. Characterization of the catalyst

The XRD pattern of the synthesized passivated carbide (Fig. 1a) corresponds to the diffraction of the hexagonal compact phase (hcp) β-Mo_2C structure. As can be observed, new phases were not detected after the catalytic run in the presence of sulfur (Fig. 1b). The small peak at around $2\theta = 36°$ corresponds to the diffraction line of SiC, i.e., residue of the carborundum (SiC) mixed with the catalyst, as described in section 2.6.

HRTEM showed that no MoS_2 slabs could be observed in the sample used under the conditions of the HDN catalytic run, in agreement with the work of Da Costa et al. [11]. However, the presence of sulfide species in the composition of the active sites cannot be ruled out [33,34].

The specific surface area of the molybdenum carbide was 33 m^2 g^{-1} and CO titration led to 142 µmol of CO chemisorbed per gram of sample. Assuming [3,28–32,35] that one CO molecule titrates only one molybdenum atom with metallic properties and that the average density of surface molybdenum atoms on an hcp β-Mo_2C is 1 ×

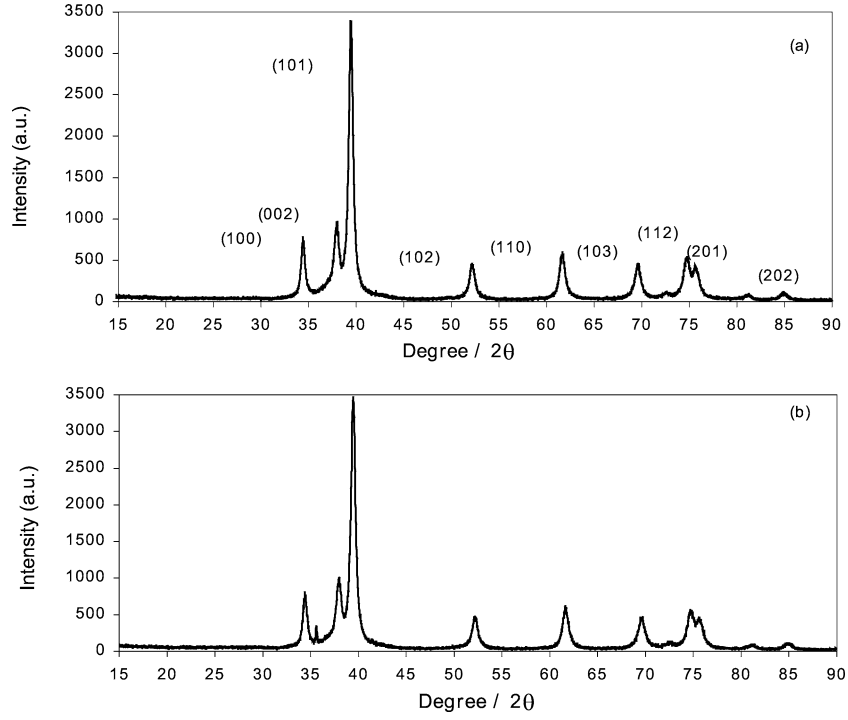

Fig. 1. X-ray diffraction pattern of bulk molybdenum carbide (β-Mo_2C): (a) before catalytic run; (b) after catalytic run.

Table 1
Distribution of intermediates and products (mol%) during the HDN of carbazole over bulk β-Mo_2C at 613 K, 6 MPa, and $t_c = 0.27$ s

	mol%
1. Nitrogen-containing compounds (Fig. 2)	
Tetrahydrocarbazole (THC)	13
Orthocyclohexylaniline (OCHA)	1
2. Direct denitrogenation (DDN, route 1, Fig. 2)	
Biphenyl (BPh)	0
3. Direct denitrogenation (DDN, route 2, Fig. 2)	
Cyclohexylbenzene (CHB)	6
4. Hydrogenation (HYD, route 3, Fig. 2)	
Cyclohexyl-cyclohexene (CHCHe)	1
Bicyclohexyl (BCH)	22
5. Isomerization	
$\sum$ isomers of CHB and BCH	29
Carbazole conversion (%)	72
HDN conversion (%)	58

10^{15} Mo cm^{-2}, it is calculated that 26% of the surface molybdenum atoms were exposed as metallic sites on the synthesized carbide [31].

3.2. Distribution of products and intermediates: reaction network of the HDN of carbazole over bulk molybdenum carbide

Table 1 illustrates all the products and intermediates observed for a run conducted at 613 K, with a contact time of 0.27 s, a HDN conversion of 58%, and a total carbazole conversion of 72%. Higher conversions were obtained but did not enable us to detect all the intermediates involved in the HDN carbazole reaction pathway.

Products are divided into five groups: N-containing compounds, biphenyl from the direct denitrogenation (route 1, Fig. 2), cyclohexylbenzene from the direct denitrogenation (route 2, Fig. 2), cyclohexyl-cyclohexene and bicyclohexyl according to the hydrogenation (route 3, Fig. 2), and isomerization products.

The hydrogenated nitrogen product tetrahydrocarbazole (THC) was detected in a significant amount (13 mol%). Successive hydrogenated carbazole compounds, such as hexahydrocarbazole, octahydrocarbazole, decahydrocarbazole, and perhydrocarbazole, were not detected under our operating conditions due to their high reactivity, in agreement with the work of Miyao et al. [23]. Orthocyclohexylaniline (OCHA) was randomly observed due to its low concentration, depending on both contact time and temperature. The major denitrogenation product was bicyclohexyl (BCH, 22 mol%, route 3, Fig. 2), with a small amount (1 mol%) of the intermediate cyclohexyl-cyclohexene (CHCHe) and 6 mol% of cyclohexylbenzene (CHB) through route 2 (Fig. 2). Side reactions, such as the isomerization of bicyclohexyl (BCH) to C_6-cyclohexyl isomers and methylcyclopentylcyclohexane, as well as the isomerization of cyclohexylbenzene (CHB)

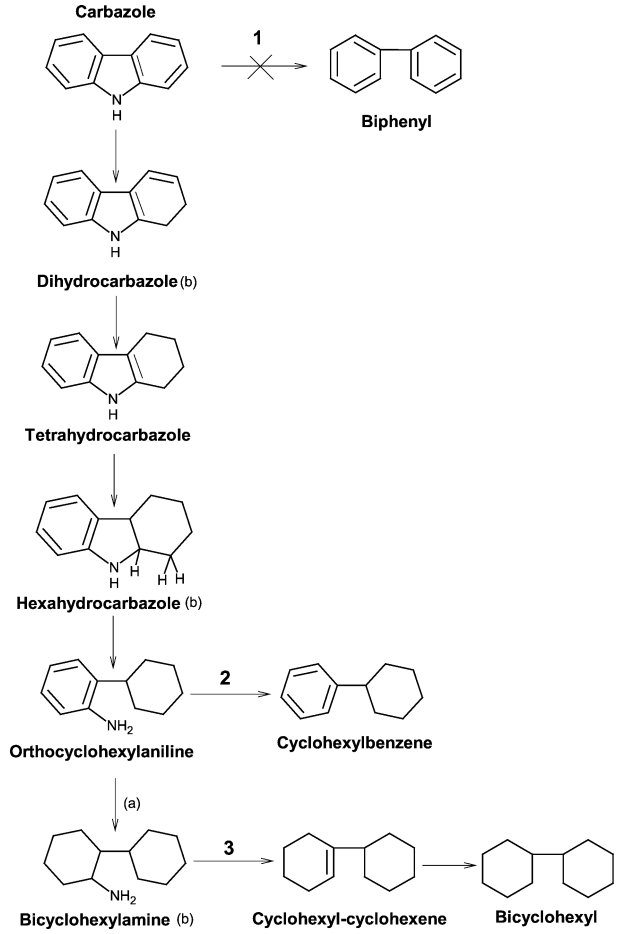

Fig. 2. Reaction pathway of the HDN of carbazole over bulk β-Mo_2C: (a) global step of hydrogenation; (b) undetected products. Acronyms: tetrahydrocarbazole (THC), orthocyclohexylaniline (OCHA), cyclohexylbenzene (CHB), cyclohexyl-cyclohexene (CHCHe), and bicyclohexyl (BCH).

to $n$$C_6$-benzene, cyclopentyl-phenyl methane, and methylcyclopentylbenzene occurred on this catalyst (29 mol%).

In accordance with the products observed, a reaction scheme of the HDN of carbazole over bulk molybdenum carbide is proposed in Fig. 2. For the sake of clarity, side reactions are not reported but three very reactive intermediates are indicated in the reaction pathway (Fig. 2, products labeled (b)). These latter intermediates are probably formed as C(sp^3)–N bond breaking is more favored than C(sp^2)–N bond breaking [21]. Carbazole is hydrogenated to dihydrocarbazole (DiHC) and then to THC, which very likely undergoes partial hydrogenation prior to the hydrogenolysis of the C(sp^3)–N bond to form OCHA. Then, from OCHA, kinetic coupling takes place and the subsequent reactions can occur either through the denitrogenation pathway (DDN, route 2, Fig. 2) to give CHB as a product or through the hydrogenation pathway (HYD, route 3, Fig. 2), leading to CHCHe and finally to BCH. Routes 2 and 3 are, thus, parallel reactions. Hydrogenation of CHB to BCH is not favored as long as nitrogen-containing compounds are still present in the feed.

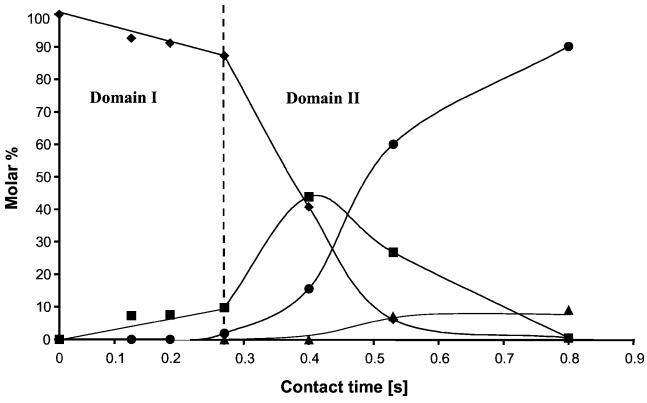

Fig. 3. Distribution of reactant, intermediates, and products observed during the HDN of carbazole versus contact time over bulk β-Mo_2C at 573 K: (♦) carbazole, (■) tetrahydrocarbazole (THC), (▲) cyclohexylbenzene (CHB), and (●) bicyclohexyl (BCH).

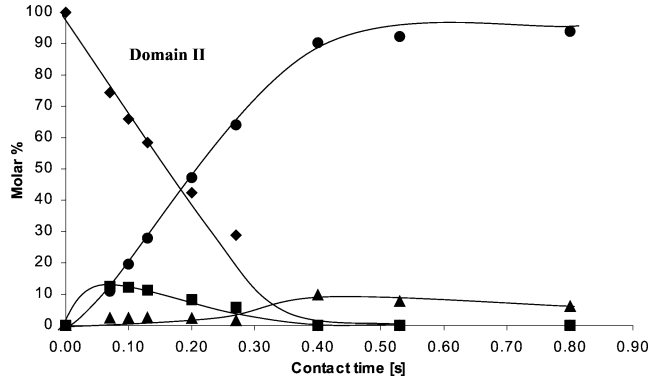

Fig. 4. Distribution of reactant, intermediates, and products observed during the HDN of carbazole versus contact time over bulk β-Mo_2C at 633 K: (♦) carbazole, (■) tetrahydrocarbazole (THC), (▲) cyclohexylbenzene (CHB), and (●) bicyclohexyl (BCH).

This is due to competitive adsorption, as observed in HDS reactions [36–38].

The product of the direct denitrogenation pathway (DDN, route 1, Fig. 2), i.e., biphenyl (BPh), was not observed in our study over bulk molybdenum carbide, whatever the operating conditions. The absence of this DDN pathway was also reported by Nagai et al. [4,23,39–41] in the HDN of carbazole *in the absence of H_2S* over similar catalysts, mainly bulk and supported molybdenum nitride. This is an interesting result because the DDS pathway corresponding to this DDN pathway (route 1, Fig. 2) was observed over bulk molybdenum carbide for the hydrodesulfurization of dibenzothiophene, which is the sulfur-containing compound corresponding to carbazole [42].

3.3. Kinetic results

To study the kinetics of the carbazole HDN reactions, the molar percentages of the reactant, intermediates, and products were plotted versus contact time for various temperatures, as shown, for example, in Fig. 3 (573 K) and Fig. 4 (633 K). Both these figures are representative of the two types of plots observed during the kinetic study of the HDN of carbazole. The profiles of these plots depend on the temperature of the process (see for example Fig. 5 for carbazole consumption). The following sections discuss the effect of temperature ($T < 613$ K and $T > 633$ K) on the kinetics of the HDN of carbazole for each type of compound: the reactant (carbazole), the main intermediate (THC), and the denitrogenated products (BCH, CHB, CHCHe, and their corresponding isomers).

3.3.1. Low temperatures ($T < 613$ K)

Fig. 3 is representative of runs conducted below 613 K; two distinct domains can be observed: domain I for $t_c < 0.27$ s and domain II for $t_c > 0.27$ s. In the latter domain, the curves behave as if the reaction pathway consists of successive reactions. The reactant (carbazole) concentration decreases, while the THC concentration reaches a maximum and, finally, the product concentrations (BCH, CHB) increase with contact time.

In domain I ($t_c < 0.27$ s), the carbazole concentration decreases linearly. This means that carbazole saturates most of the free active sites of the catalyst. Consequently, the number of free pairs of adjacent active sites is too small to proceed to the dissociation of dihydrogen (following a Polanyi–Horiuti mechanism) and the carbazole conversion is very low. In domain I, both reaction rates (consumption of carbazole and formation of THC) are equal. This rate corresponds to the hydrogenation of carbazole to THC (Fig. 2).

For $t_c > 0.27$ s (domain II), the carbazole conversion increases and consequently the carbazole coverage must slightly decrease, the rate of consumption of carbazole still being constant. Therefore, a sufficient number of pairs of adjacent active sites becomes free, allowing H_2 to dissociate and to speed up the reaction. The conversion of carbazole increases significantly, from 10 to 80%, within a narrow range of contact times ($0.27 < t_c < 0.47$ s). Moreover, since the decrease in the carbazole concentration versus contact time is *linear* up to 80% conversion, a true zero-order reaction with respect to carbazole must be considered. As no partially hydrogenated nitrogen compounds (such as hexa-, octa-, deca-, perhydrocarbazole, bicyclohexylamine) were detected, it means that they are probably very reactive and at a very low concentration on the surface. Consequently, adsorbed carbazole must be considered as the most abundant reaction intermediate (*mari*) according to Boudart's concept [43] and the following balance on active sites can be considered:

$$[\mathrm{L}] \sim [{}^*\text{carbazole}], \tag{1}$$

where [L] is the density of sites and [*carbazole] the adsorbed carbazole concentration. Therefore, the rate of disappearance of carbazole (r_d) is

$$r_d = k[{}^*\text{carbazole}] \sim k[\mathrm{L}] = \text{constant} = k', \tag{2}$$

considering a one-way elementary step for carbazole hydrogenation and k as the corresponding rate constant.

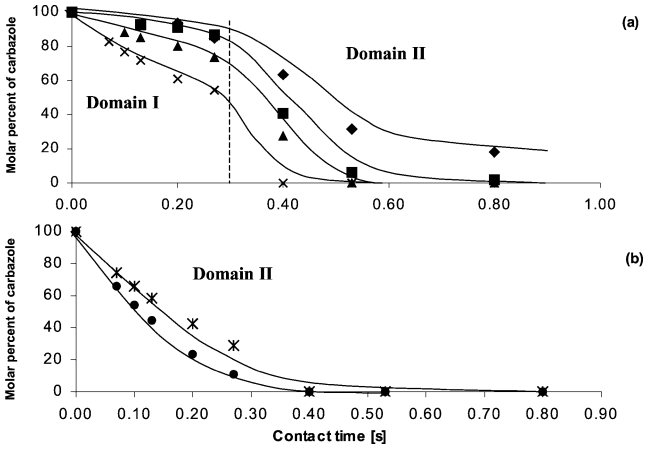

Fig. 5. Molar percent of carbazole versus contact time during the HDN of carbazole over bulk β-Mo_2C. (a) Low-temperature range: (♦) 553 K, (■) 573 K, (▲) 593 K, and (×) 613 K. (b) High-temperature range: (∗) 633 K and (●) 653 K.

Under our operating conditions, HDN conversion reaches 100% for a contact time as low as 0.8 s.

Fig. 5 presents the disappearance of carbazole versus contact time and temperature. It indicates that the two-domain profile is indeed observed when the temperature is below 613 K (see Fig. 5a at 553, 573, 593, and 613 K). In domain I, the saturation of the active sites by carbazole is too high for the reaction to proceed (as explained previously). As expected, when the temperature increases (Fig. 5b at 633 and 653 K), domain I is no longer observed due to a higher carbazole conversion and to the presence of free pairs of active sites, leading to the dissociation of H_2 (as explained previously).

For $t_c < 0.27$ s (domain I), the concentration of THC is low, in agreement with carbazole conversion. For $t_c > 0.27$ s (domain II), THC behaves as an intermediate as it passes through a maximum (45 mol% at 0.4 s). Up to $t_c = 0.4$ s, THC increases and also reacts to BCH. For $t_c > 0.4$ s, THC starts to decrease and leads to both BCH and CHB; it disappears completely at $t_c = 0.8$ s. The molar percentage of HDN products (BCH + CHCHe + isomers from route 3 and CHB + isomers from route 2) is presented versus contact time in Fig. 3. The major product of the reaction was BCH. Its concentration increases with contact time, concurrently with the decrease in the carbazole and THC concentrations. At $t_c = 0.8$ s, when no more nitrogen compounds are present, the selectivity between routes 3 and 2 can be calculated from the ratio of their respective concentration products; it is equal to 9. The DDN pathway (route 2) is not as favored as the HYD pathway (route 3).

3.3.2. High temperatures ($T > 633$)

Fig. 4 represents a run conducted at 633 K. It is representative of runs conducted at temperatures higher than 633 K; only domain II is observed. Indeed, at such temperatures, the conversion is substantial, even at very short contact times. At 633 K, the decrease in carbazole is linear up to 60% conversion. The zero-order reaction with respect to carbazole is observed once again. At a contact time of 0.4 s, carbazole conversion is already complete. At 653 K, the decrease in carbazole is not linear (Fig. 5). Since the catalyst is more active at the higher temperature, the carbazole consumption rate increases and the surface is no longer saturated by the reactant.

Above 633 K, the concentration of THC goes through a maximum, which is, however, smaller (13 mol%) than that at 573 K (Fig. 3) as well as at a shorter contact time (around 0.07 s). The conversion of carbazole is higher and the concentration of the intermediate decreases as it is quickly transformed to products. Finally, at $t_c = 0.4$ s, no THC is observed and the HDN conversion reaches 100%.

As described above, BCH is the major product, while the concentration of CHB remains very low (8 mol% for $t_c = 0.4$ s). The concentration of BCH increases linearly as carbazole decreases, and the rate of formation of BCH is similar to the rate of the disappearance of carbazole. At $t_c = 0.4$ s, the selectivity ratio between routes 3 and 2 (Fig. 2) is equal to 9. Route 3 (HYD pathway) is still favored over route 2 (DDN pathway) at the higher temperature. Above 0.4 s, when nitrogen compounds are no longer present, a slight hydrogenation of CHB to BCH is observed (CHB concentration decreases).

3.3.3. Detailed kinetic study of HDN of carbazole

At 633 K (Fig. 4) and between 0.07 and 0.27 s, the rates of the hydrogenation of carbazole and of the formation of BCH are constant and are approximately equal to 220 and 233 s^{-1}, respectively. In this range of contact times, less than 10 mol% THC is present in the product. Thus, the major global reaction seems to be at 633 K:

$$\text{Carbazole} + 9H_2 = \text{BCH} + NH_3. \quad (3)$$

This is quite different from the situation over a commercial sulfided CoMo or NiMo alumina-supported catalyst [44,45].

The general pathway in Fig. 2 can then be simplified to the catalytic cycle shown in Fig. 6. For the sake of simplicity, a *global* hydrogenation step is included between *OCHA and *BCHA. This is possible because the hydrogen pressure is in excess and remained more or less constant throughout the reaction.

As is often the case in catalysis, one of the intermediates can desorb before reacting on the surface, depending on the corresponding rate constants:

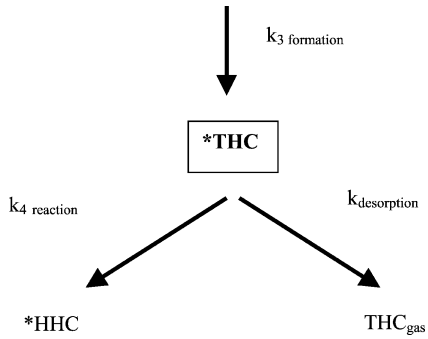

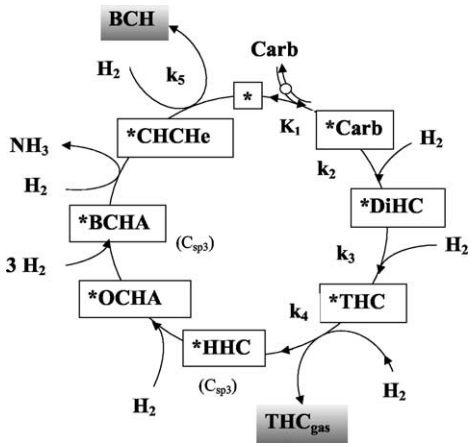

Fig. 6. Major catalytic cycle at 633 K for the global reaction: carbazole + $9H_2$ = BCH + NH_3 according to the data presented in Fig. 4. Carb, carbazole; DiHC, dihydrocarbazole; THC, tetrahydrocarbazole; HHC, hexahydrocarbazole; OCHA, orthocyclohexylaniline; BCHA, bicyclohexylaniline; CHCHe, cyclohexylcyclohexene; BCH, bicyclohexyl.

(rate constants are defined according to Fig. 6). If $k_{\text{desorption}} > k_{4\,\text{reaction}}$, then a fraction of THC can desorb before being hydrogenated to *HHC. In the opposite case, if $k_{\text{desorption}} < k_{4\,\text{reaction}}$, there is no chance for the intermediate to desorb as it is quickly transformed. This explains why DiHC, HHC, and BCHA were not detected.

In the catalytic cycle (Fig. 6) all the elementary steps turn over at the same rate. If an i-elementary step occurs σ_i times in the cycle to obtain the global reaction, represented by Eq. (3), the turnover rate is equal to $r_{i,\text{net}}/\sigma_i$, σ_i being the *stoichiometric number* [43]. In the present case, σ_i is always equal to unity, and the rate of reaction can be written as

$$r = k_2[{}^*\text{carbazole}] = k_5[{}^*\text{CHCHe}] = k_2[\text{L}]$$
$$= k_{\text{exp}}(\text{zero order with respect to carbazole}).$$

The cycle (Fig. 6) is kinetically equivalent to the following two-step catalytic reactions [43]:

$$\text{Carb} + {}^* \overset{K_1}{\rightleftharpoons} {}^*\text{Carb}, \tag{4}$$

$${}^*\text{Carb} + \text{H}_2 \overset{k_2}{\longrightarrow} \cdots \tag{5}$$

with [*carbazole] = [L]. Therefore, the rate-determining step (Eq. (5)) leads to

$$r = k_2[{}^*\text{carbazole}] = k_2[\text{L}] = k_{\text{exp}}.$$

The Arrhenius plot, $\ln k_{\text{exp}}$ versus $1/T$, applied in domain II, permits calculation of the activation energy corresponding to the rate constant k_2.

The slopes of the carbazole curves were determined in domain II between 553 and 633 K (Figs. 5a and 5b). The energy of activation of the reaction, defined above, can be calculated from the Arrhenius plot (Fig. 7); it is equal to 86.6 kJ mol^{-1}. This value is in agreement with the activation energy of the hydrogenation of such nitrogen-containing aromatic compounds [46]. This result is consistent with the rate-determining step (Eq. (5)).

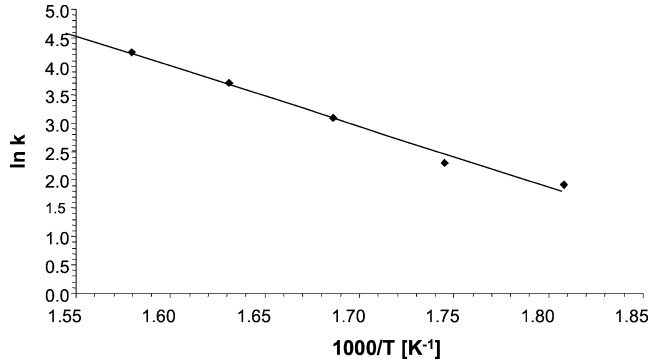

Fig. 7. Arrhenius plot of the carbazole hydrogenating step.

4. Conclusion

The present study shows that *bulk* molybdenum carbide is active in the HDN of carbazole in the presence of a small amount of sulfur (50 ppm). This sulfur concentration corresponds to the 2005 European regulations. Under such an atmosphere, no MoS_2 slabs were detected by HRTEM. The direct denitrogenation pathway of carbazole transformation (route 1, Fig. 2), leading to biphenyl, was not observed on the *bulk* molybdenum carbide, in contrast to commercial hydrotreating catalysts. The main product of HDN of carbazole was bicyclohexyl (route 3, Fig. 3). The kinetic study showed that a minimum contact time (0.27 s) or temperature (633 K) is required to proceed to a substantial conversion and to the complete disappearance of carbazole and tetrahydrocarbazole. For $t_c < 0.27$ s and $T < 633$ K, a first domain is observed (domain I) in which the HDN conversion of carbazole is low, due to a high carbazole coverage and, consequently, to a low hydrogen coverage, preventing the HDN reaction to proceed. When the contact time is increased, the HDN reaction of carbazole starts; the hydrogen coverage is higher and a second domain (II) is observed. Furthermore, if the temperature is increased ($T > 633$ K), only domain II remains for the whole range of contact times, and a substantial reaction rate is reached. At 633 K, a zero-order reaction is observed with respect to carbazole, and the selectivity ratio between routes 3 and 2 is equal to 9. A detailed kinetic analysis is given. The rate-determining step is the first carbazole hydrogenation step, in agreement with the corresponding experimental energy of activation.

Acknowledgments

We greatly acknowledge the French National Center for Scientific Research (CNRS), the Polish Academy of Science (PAN) and Science Committee (KBN), the French Foreign Office (Warsaw French Ambassy), and TotalFinaElf for their financial support in the Framework of the PICS 508 and Jumelage “Materials for environment.”

References

[1] R. Prins, Adv. Catal. 46 (2001) 399.
[2] J.S. Lee, M. Boudart, Appl. Catal. 19 (1985) 207.
[3] J.C. Schlatter, S.T. Oyama, J.E. Metcalfe III, J.M. Lambert Jr., Ind. Eng. Chem. Res. 27 (1988) 1648.
[4] M. Nagai, T. Miyao, Catal. Lett. 15 (1992) 105.
[5] C.C. Yu, S. Ramanathan, F. Sherif, S.T. Oyama, J. Phys. Chem. 98 (1994) 13038.
[6] V. Schwartz, V.L.T. Da Silva, J.G. Chen, S.T. Oyama, Stud. Surf. Sci. Catal. A 130 (2000) 467.
[7] J.G. Choi, J.R. Brenner, C.W. Colling, B.G. Demczyk, J.L. Dunning, L.T. Thompson, Catal. Today 15 (1992) 201.
[8] K.S. Lee, H. Abe, J.A. Reimer, A.T. Bell, J. Catal. 139 (1993) 34.
[9] J.G. Choi, J.R. Brenner, L.T. Thompson, J. Catal. 154 (1995) 33.
[10] S. Ramanathan, S.T. Oyama, J. Phys. Chem. 99 (1995) 16365.
[11] P. Da Costa, J.L. Lemberton, C. Potvin, J.M. Manoli, G. Perot, M. Breysse, G. Djéga-Mariadassou, Catal. Today 65 (2001) 195.
[12] J.S. Lee, M.H. Yeom, K.Y. Park, I.S. Nam, J. Catal. 128 (1991) 126.
[13] M. Nagai, T. Miyao, T. Tuboi, Catal. Lett. 18 (1993) 9.
[14] C.W. Colling, L.T. Thompson, J. Catal. 146 (1994) 193.
[15] B. Dhandapani, S.T. Oyama, Catal. Lett. 35 (1995) 353.
[16] D. Mordenti, D. Brodzki, G. Djéga-Mariadassou, J. Solid State Chem. 141 (1998) 114.
[17] B. Dhandapani, S. Ramanathan, C.C. Yu, B. Frühberger, J.G. Chen, S.T. Oyama, J. Catal. 176 (1998) 61.
[18] J. Trawczynski, Catal. Today 65 (2001) 343.
[19] C. Sayag, S. Suppan, J. Trawczynski, G. Djéga-Mariadassou, Fuel Process. Technol. 77–78 (2002) 261.
[20] J.R. Katzer, R. Sivasubramaniam, Catal. Rev. Sci. Eng. 20 (1979) 155.
[21] G. Perot, Catal. Today 10 (1991) 447.
[22] M.J. Ledoux, A. Bouassida, R. Benazouz, Appl. Catal. 9 (1984) 41.
[23] T. Miyao, K. Oshikawa, S. Omi, M. Nagai, Stud. Surf. Sci. Catal. 106 (1997) 255.
[24] C.N. Satterfield, M. Modell, J.F. Mayer, AIChE 21 (1975) 1100.
[25] M. Nagai, T. Kabe, J. Catal. 81 (1983) 440.
[26] V. LaVopa, C.N. Satterfield, J. Catal. 110 (1988) 375.
[27] P. Del Gallo, C. Pham-Huu, A.P.E. York, M.J. Ledoux, Ind. Eng. Chem. Res. 35 (1996) 3302.
[28] L. Volpe, M. Boudart, J. Solid State Chem. 59 (1985) 348.
[29] D.J. Sajkowski, S.T. Oyama, Appl. Catal. A 134 (1996) 339.
[30] C. Sayag, G. Bugli, P. Havil, G. Djéga-Mariadassou, J. Catal. 167 (1997) 372.
[31] J.S. Choi, G. Bugli, G. Djéga-Mariadassou, J. Catal. 193 (2000) 238.
[32] E.I. Ko, R.J. Madix, Surf. Sci. 109 (1981) 221.
[33] P.A. Aegerter, W.W.C. Quigley, G.J. Simpson, D.D. Ziegler, J.W. Logan, K.R. McCrea, S. Glazier, M.E. Bussell, J. Catal. 164 (1996) 109.
[34] R.R. Chianelli, G. Berhault, Catal. Today 53 (1999) 357.
[35] G.S. Ranhotra, G.W. Haddix, A.T. Bell, J.A. Reimer, J. Catal. 108 (1987) 24.
[36] L.D. Rollman, J. Catal. 46 (1977) 243.
[37] P. Michaud, J.L. Lemberton, G. Pérot, Appl. Catal. A 169 (1998) 343.
[38] P. Da Costa, C. Potvin, J.M. Manoli, J.L. Lemberton, G. Pérot, G. Djéga-Mariadassou, J. Mol. Catal. A: Chem. 184 (2002) 323.
[39] M. Nagai, Y. Goto, A. Irisawa, S. Omi, J. Catal. 191 (2000) 128.
[40] M. Nagai, Y. Goto, O. Uchino, S. Omi, Catal. Today 43 (1998) 249.
[41] M. Nagai, Y. Goto, A. Miyata, M. Kiyoshi, K. Hada, K. Oshikawa, S. Omi, J. Catal. 182 (1999) 292.
[42] H.K. Park, D.S. Kim, K.L. Kim, Korean J. Chem. Eng. 15 (1998) 625.
[43] M. Boudart, G. Djéga-Mariadassou, Kinetics of Heterogeneous Catalytic Reactions, Princeton University Press, Princeton, NJ, 1984.
[44] H. Schulz, M. Shon, N.M. Rahman, Stud. Surf. Sci. Catal. 27 (1986) 201.
[45] Z. Sarbak, Acta Chim. Hung. 127 (1990) 359.
[46] J. Shabtai, G.J.C. Yeh, C. Russel, A.G. Oblad, Ind. Eng. Chem. Res. 28 (1989) 139.